Published in final edited form as:
Biochemistry. 2012 January 24; 51(3): 820–828. doi:10.1021/bi201731p.

Factor VIII Light Chain Contains a Binding Site for Factor X That Contributes to the Catalytic Efficiency of Factor Xase†

Masahiro Takeyama, **Hironao Wakabayashi**, and **Philip J. Fay***
Department of Biochemistry and Biophysics, University of Rochester School of Medicine and Dentistry, 601 Elmwood Avenue, Rochester, NY 14642, USA

Abstract

Factor (F) VIII functions as a cofactor in FXase, markedly accelerating the rate of FIXa-catalyzed activation of FX. Earlier work identified a FX-binding site having μM affinity within the COOH-terminal region of the FVIIIa A1 subunit. In the present study, surface plasmon resonance (SPR), ELISA-based binding assays and chemical cross-linking were employed to assess an interaction between FX and the FVIII light chain (A3C1C2 domains). SPR and ELISA-based assays showed that FVIII LC bound to immobilized FX (K_d = 165 nM and 370 nM, respectively). Furthermore, active site-modified activated protein C (DEGR-APC) effectively competed with FX in binding FVIII LC (apparent K_i = 82.7 nM). Western blotting revealed that the APC-catalyzed cleavage rate at Arg^{336} was inhibited by FX in a concentration-dependent manner. A synthetic peptide comprising FVIII residues 2007–2016 representing a portion of an APC-binding site blocked the interaction of FX and FVIII LC (apparent K_i = 152 μM) and directly bound to FX (K_d = 7.7 μM) as judged by SPR and chemical cross-linking. Ala-scanning mutagenesis of this sequence revealed that the A3C1C2 subunit derived from FVIII variants Thr2012Ala and Phe2014Ala showed 1.5- and 1.8-fold increases in K_d for FX, whereas this value using the A3C1C2 subunit from a Thr2012Ala/Leu2013Ala/Phe2014Ala triple mutant was increased >4-fold. FXase formed using this LC triple mutant demonstrated an ~4-fold increase in the K_m for FX. These results identify a relatively high affinity and functional FX site within the FVIIIa A3C1C2 subunit and show a contribution of residues Thr2012 and Phe2014 to this interaction.

FVIII[1] functions as a cofactor for FIXa in the enzyme complex termed FXase that is responsible for the anionic phospholipid surface-dependent conversion of FX to FXa (1). FVIII is synthesized as an ~300 kDa precursor with the domain structure A1-A2-B-A3-C1-C2. This precursor is processed to a series of divalent metal ion-dependent heterodimers by cleavage at the B-A3 junction, generating a HC (2) consisting of the A1A2B domains and a LC consisting of the A3C1C2 domains (3–5). The procofactor FVIII is activated by cleavage at Arg^{372}, Arg^{740}, and Arg^{1689} by either thrombin or FXa, converting the dimer into the FVIIIa trimer composed of the A1, A2, and A3C1C2 subunits (6). Proteolysis at Arg^{372} and Arg^{1689} is essential for generating FVIIIa cofactor activity. Cleavage at the

†This work was supported by National Institutes of Health Grants HL76213 and HL38199. M.T. acknowledges support from the SENSHIN Medical Research Foundation.

*To whom correspondence should be addressed: Department of Biochemistry and Biophysics, University of Rochester School of Medicine and Dentistry, 601 Elmwood Avenue, Rochester, NY 14642, USA. Tel.: 585-275-6576; Fax: 585-275-6007; philip_fay@urmc.rochester.edu.

[1]Abbreviations: F, factor; LC, light chain; HC, heavy chain; VWF, von Willebrand factor; APC, activated protein C; RVV-X, FX activator in Russell's viper venom; DEGR, 1,5-dansyl-Glu-Gly-Arg; SDS-PAGE, sodium dodecyl sulfate-polyacrylamide gel electrophoresis; EDC, 1-ethyl-3-(3-dimethylaminopropyl)-carbodiimide hydrochloride; HEPES, 4-(2-hydroxyethyl)-1-piperazineethanesulfonic acid; PBS, phosphate-buffered saline; HBS, Hepes-buffered saline; CAPS, 3-(cyclo-hexylamino)-1-propanesulfonic acid; SPR, surface plasmon resonance; ELISA, enzyme-linked immunoadsorbent assay; BSA, bovine serum albumin; PVDF, polyvinylidene difluoride

former site exposes a functional FIXa-interactive site within the A2 domain that is cryptic in the unactivated molecule (7). Cleavage at the latter site liberates the cofactor from its carrier protein, VWF (8) contributing to the overall specific activity of cofactor (9). FXa also inactivates FVIIIa following cleavages at Arg^{336} (6) and Lys^{36} (10) within the A1 subunit. Inactivation following cleavage at Arg^{336} likely occurs by altered interaction of the A2 subunit with the truncated A1 (11) coupled with an increase in the K_m for substrate FX (12), the latter reflecting loss of a FX-interactive site within an acidic residue-rich region defined by residues 337–372 (13). Other proteases including activated protein C (APC) (6) and FIXa have been shown also to attack this site (14).

APC is a potent anticoagulant that proteolytically inactivates FVIIIa and FVa, in surface-dependent reactions (15). APC inactivates FVIIIa by cleaving the A1 subunit at Arg^{336} and A2 subunit at Arg^{562} (16, 17). APC binds the LC subunit of the cofactors (18, 19) at a region localized to the C-terminal end of the A3 domain (residues 2007–2016) (20).

Earlier work from our laboratory identified a FX-binding site having μM affinity within the C-terminal acidic region of the FVIIIa A1 subunit (13). However, the contribution of FVIII LC (A3C1C2 domains) to binding FX was not determined. In the present study, we demonstrate by solid phase binding assays and chemical cross-linking that FX binds to FVIII LC. Competition of FX binding by APC and a peptide prepared from the APC-binding site in FVIII LC suggest that the FX site overlapped with a site for APC. Furthermore, mutagenesis of residues within this FVIII sequence residues Thr2012 and Phe2014 as contributing to the FX binding interaction and to the K_m of FXase for FX.

MATERIALS AND METHODS

Reagents

Recombinant FVIII (Kogenate ™) and the monoclonal antibodies 58.12 and 2D2 recognizing the N-terminal end of the A1 domain and the A3 domain, respectively, were generous gifts from Dr Lisa Regan of Bayer Corporation (Berkeley, CA). An anti-C2 monoclonal antibody (GMA-8003) and an anti-human FX monoclonal antibody (GMA-520) were obtained from Green Mountain Antibodies (Burlington, VT). Antibody 10104, a monoclonal antibody that binds the N-terminal region of FVIII LC, was obtained from QED Bioscience Inc. (San Diego, CA). The reagents human α-thrombin, RVV-X, FXa, human APC and human APC - DEGR (Hematologic Technologies Inc., Essex Junction, VT), FIXa and FX (Enzyme Research Laboratory, South Bend, IN), hirudin (DiaPharma, West Chester, OH), the chromogenic Xa substrate (Centerchem Inc., Norwalk, CT), S-2222 (Chromogenix, Lexington, MA), TENSTOP™ (American Diagnostica Inc. Stanford, CT), and EDC (Pierce, Rockford, IL) were purchased from the indicated vendors. Phospholipid vesicles (40% phosphatidylcholine (PC), 40% phosphatidylethanolamine (PE), and 20% phosphatidylserine (PS)) were purchased from Avanti Polar Lipids (Alabaster, AL). A synthetic peptide corresponding to FVIII A3 residues 2007–2016, a biotinylated 2007–2016 peptide, and a scrambled sequence version of this peptide were obtained from Biomatik (Wilmington, DE).

Mutagenesis, Expression and Purification of Wild Type and Variant FVIII

Recombinant wild type FVIII, as well as FVIII variants Met2010Ala, Ser2011Ala, Thr2012Ala, Leu2013Ala, Phe2014Ala, Leu2015Ala, Val2016Ala, Thr2012Ala/Phe2014Ala were constructed, expressed, and purified as described previously (21). Resultant FVIII forms were typically >90% pure as judged by SDS-PAGE with albumin representing the major contaminant. FVIII concentrations were measured using an enzyme-linked immunoadsorbent assay (ELISA) and FVIII activities were determined by one-stage

clotting assay and a two-stage chromogenic FXa generation assays. FVIII samples were quick-frozen and stored at −80 °C.

Preparation of FVIII Subunits

FVIII LC (22), A2 and A3C1C2 subunits (23) were isolated as previously described. A2/A3C1C2 complex was prepared by incubating A2 (100 nM) and A3C1C2 (10 nM), purified from WT and mutant FVIII with 20 μM PSPCPE vesicles for 10 minutes at 23 °C.

ELISA for Binding of FVIII LC to Immobilized FX

Microtiter wells were coated with FX (50 nM) in 20 mM Tris and 0.15 M NaCl, pH 7.4 (Tris-buffered saline; TBS), overnight at 4 °C. The wells were washed with Hepes-buffered saline (HBS)-buffer (20 mM HEPES, pH 7.2, 0.05 M NaCl, 0.01% Tween 20) and were blocked with HBS-buffer containing 10% skim milk for 2 hours at room temperature. Various amounts of the FVIII LC were then added in HBS-buffer containing 2 mM $CaCl_2$ and 0.01% BSA for 2 hours at 37 °C. The wells were washed with HBS-buffer and bound FVIII LC was quantified by the addition of biotinylated anti-FVIII LC monoclonal antibody, 10104 (10 μg/ml), and *O*-phenylenediamine dihydrochloride substrate (0.4 mg/ml) (24). Reactions were quenched by the addition of equal volume of 2 M H_2SO_4, and absorbance values at 493 nm were measured using a microplate reader. The amount of non-specific binding of anti-FVIII LC monoclonal antibody in the absence of FX was <5% of the total signal. Specific binding was recorded after subtracting the non-specific binding.

FX Binding to FVIII LC as Determined by FXa Generation

Methods used a modification of the procedure described (13). Microtiter wells were coated with 0.5 μg of monoclonal antibody (GMA-8003) per well in 50 μl buffer (35 mM $NaHCO_3$, 15 mM Na_2CO_3, pH 9.6) overnight at 4 °C. The wells were washed with phosphate-buffered saline (PBS) containing 0.01% Tween 20 and were blocked with PBS containing 10% skim milk for 2 hours at room temperature. FVIII LC (200 nM) and various amounts of FX (0–100 nM) in 50 μl HBS-buffer containing 2 mM $CaCl_2$ and 0.01% BSA were added to the wells. Samples were incubated for 2 hours at 37 °C, then wells were rapidly washed 5 times with 200 μl of HBS-buffer (total wash duration was less than 1 minute). Subsequently, RVV-X activator enzyme (200 ng/well) in 50 μl buffer (20 mM Tris, 200 mM NaCl, 5mM CaCl2, pH 7.2) was added and incubated for 15 minutes at room temperature, followed by the addition of the FXa-specific chromogenic substrate, S-2222 (0.46 mM final concentration) to the wells. Reactions were read at 405 nm using a microplate reader.

FXa Generation Assay

The rate of conversion of FX to FXa was monitored in a purified system (25). FVIII (1 nM) in buffer (20 mM HEPES, 0.1 M NaCl, 5 mM $CaCl_2$, pH 7.2, 0.01% Tween 20) containing 20 μM PSPCPE vesicles was activated by the addition of thrombin (30 nM). Thrombin activity was inhibited after 1 minute by the addition of hirudin (10 units/ml). The mixture was reacted with FIXa (40 nM) for 30 seconds, and then various amounts of FX were added to initiate reactions. The reactions were quenched after 1 minute by adding 50 mM EDTA. Amounts of FXa generated were determined by addition of the chromogenic substrate, S-2222 (0.46 mM final concentration) and rate of FXa generation were calculated. All reactions were run at 23 °C.

Real-time Biomolecular Interaction Analysis

The kinetics of FX interaction with FVIII LC were determined by SPR-based assay at 37 °C using BIAcore T-100 instrument (GE Healthcare, Uppsala, Sweden). FX was covalently coupled to the surface of a CM5 chip. Binding (association) of FVIII LC was monitored in

HBS-buffer containing 2 mM $CaCl_2$ for 2 minutes. The dissociation of bound FVIII LC was recorded over a 2-minute period by changing the FVIII LC-containing buffer to buffer alone. The level of nonspecific binding, corresponding to FVIII LC binding to the uncoated chip, was subtracted from the signal. After each analysis, chip surfaces were regenerated by treatment with 1.3 M NaCl for 1 minute. K_d values were determined by an equilibrium method using the evaluation software provided by GE healthcare. The data were fitted to single-site binding model.

Electrophoresis and Western Blotting

SDS-PAGE was performed using 8% gels at 175 V for 50 minutes. For Western blotting, the proteins were transferred to a PVDF membrane at 100 V for 1 hour in buffer containing 10 mM CAPS [3-(cyclo-hexylamino)-1-pro-panesulfonic acid], pH 11 and 10% (v/v) methanol. Proteins were probed using indicated anti-FVIII or anti-FX monoclonal antibodies, followed by goat anti-mouse alkaline phosphatase-linked second antibody. The signal was detected using the ECF system (Amersham Biosciences), and the blots were scanned at 570 nm using a Storm 860 instrument (Molecular Devices). Densitometric scans were quantitated using Image J 1.34 (National Institute of Health, USA).

Cleavage of FVIIIa by APC

APC (2 nM) was incubated with FVIIIa (130 nM) and indicated concentrations of FX in HBS-buffer containing 2 mM $CaCl_2$ and PSPCPE (100 μM) at 37 °C. Reactions containing FX were supplemented with TENSTOP (20 μM) to eliminate proteolysis by any traces of contaminating FXa. Control reactions showed that the presence of TENSTOP had no effect on the rate of APC-catalyzed inactivation of FVIIIa in the absence of FX. Samples were taken at the indicated times, and the reactions were immediately terminated and prepared for SDS-PAGE by adding SDS-PAGE sample buffer and boiling for 3 minutes.

Cross-linking with EDC

FVIII LC (200 nM) in the presence of FX (200 nM) was reacted with various concentrations of EDC (0–5 mM) in HBS-buffer containing 2 mM $CaCl_2$ at 23 °C for 2 hours. Reactions were terminated by addition of SDS-PAGE sample buffer and boiling for 3 minutes.

Data Analyses

All experiments were performed at least three separate times, and mean values and standard deviations are shown. Comparison of mean values was performed by the Student's *t*-test. Nonlinear least squares regression analyses were performed by Kaleidagraph (Synergy, Reading, PA). Analyses of the interactions between the FX and FVIII LC measured by ELISA were performed using a single-site binding model by Equation 1,

$$Absorbance = \frac{A_{max} \cdot [S]}{K_d + [S]} \quad \text{(Eq. 1)}$$

where [S] is the concentration of FVIII LC in the solid phase binding assay, K_d is the dissociation constant, and A_{max} represents maximum absorbance signal when the site is saturated by the FVIII LC.

Data from studies assessing DEGR-APC-dependent inhibition of FX interaction with FVIII LC were fitted by nonlinear least squares regression by using competitive inhibition model,

$$\%binding = \frac{B_{\max} \cdot [L_0]}{K_d \cdot \left[1 + \frac{[L]}{K_i}\right] + [L_0]} + C \quad \text{(Eq. 2)}$$

where L represents the concentration of DEGR-APC or FX, L_0 is the concentration of FVIII LC, B_{max} represents maximum binding, K_d is the dissociation constant for the interaction between FVIII LC and FX, K_i is the apparent inhibition constant for L, and C is a constant for binding of FVIII LC and FX that was unaffected by L.

RESULTS

Interaction Between FVIII LC and FX Monitored by Solid Phase Binding Assays

Surface plasmon resonance was used to evaluate FVIII LC binding to FX. Various concentrations of FVIII LC were reacted with FX that had been immobilized onto a CM5 sensor chip. The interaction of FVIII LC with FX was of relatively low affinity (K_d = 165 ± 8 nM), thus this parameter value was determined from maximum response units (RU) following the addition of various concentrations of FVIII LC. These RU values were shown to be concentration-dependent, and the data were well-fitted to a single-site binding model (Fig 1A).

In a complementary series of experiments, the binding of FVIII LC to immobilized FX was measured using a solid-phase ELISA-based (non-equilibrium) assay. Various concentrations of FVIII LC were incubated with FX (50 nM) that had been immobilized onto microtiter wells, and bound FVIII LC was detected using a biotinylated anti-FVIII LC antibody as described in *Methods*. As shown in Fig 1B, FVIII LC binding to FX was concentration-dependent and saturable. The resultant data were well-fitted to a single-site binding model, yielding an apparent K_d value (370 ± 10 nM) approximating that value determined by SPR. In addition, a reciprocal experiment was performed where FVIII LC in the presence of various concentrations of FX was then adsorbed onto microtiter wells through use of an anti-LC capture antibody, GMA-8003. The amount of FX bound to LC adsorbed onto the well was quantitated following its conversion to FXa by the FX activator (RVV) and subsequent reaction with the FXa-specific chromogenic substrate, S-2222. FX bound to FVIII LC in a concentration-dependent manner (data not shown) yielding an apparent K_d of 89.9 ± 18.2 nM. To confirm the specificity of this binding, various concentrations of FX were reacted with FVIII LC (500 nM) in the fluid phase, prior to addition to microtiter wells containing immobilized FX. The soluble FX competed for FVIII LC binding to the immobilized FX by ~90% with an apparent K_i value (154 ± 13 nM, Fig 1B *inset*) similar to the estimated K_d. Taken together, these results indicated a specific and moderate affinity interaction between FVIII LC and FX.

Zero-length Cross-linking of FVIII LC and FX

To complement the data obtained using solid phase-based assays, the interaction of FVIII LC and FX was further demonstrated in the solution phase. Association of the two proteins was assessed using the zero-length cross-linking reagent, EDC. FVIII LC (200 nM) in the presence of FX (200 nM) was reacted with various concentrations of EDC at 23 °C for 2 hours. Following this cross-linking protocol, samples were subjected to SDS-PAGE, transferred PVDF, and probed with an anti-FVIII A3 domain monoclonal antibody (2D2, Fig 1C, panel a) or anti-FX monoclonal antibody (GMA-520, Fig 1C, panel b). FVIII LC and FX formed a cross-linked product of approximately 140 kDa that was observed with either antibody, and that increased in staining density with increasing amounts of EDC. The mass of the adduct was consistent with a 1:1 stoichiometry of FVIII LC (~80 kDa) and FX

(~59 kDa). Control experiments showed that no cross-linked product was formed between FVIII LC or FX and bovine serum albumin (data not shown).

DEGR-APC Inhibits the Interaction Between FVIII LC and FX

Earlier studies localized an APC binding site within the FVIII A3 domain (20). We examined whether active-site modified (DEGR-) APC affected the interaction between FVIII LC and FX using the ELISA-based binding assays. Various concentrations of DEGR-APC in the presence of FVIII LC (500 nM) were incubated with immobilized FX (50 nM), and bound FVIII LC was detected using a biotinylated anti-FVIII LC antibody, 10104. This antibody binds within the a3 acidic segment (residues 1649–1689) of LC (5) and thus would not be expected to alter interaction of LC with either FX or APC. DEGR-APC inhibited the binding of FVIII LC to FX in a concentration-dependent manner (Fig 2), with >80% inhibition observed at the maximum concentration of DEGR-APC employed (1 μM). An apparent K_i value of 82.7 ± 17.0 nM was estimated for DEGR-APC. These results suggested that the FX-interactive site on FVIII LC might overlap with an APC-binding site.

FX Inhibits the Proteolytic Cleavage of FVIIIa by APC

In an earlier study (26), we showed that high concentrations of FX protected FVIII from APC-catalyzed cleavage at Arg^{336}. In order to extend and quantitate that original observation, we performed an experiment where FX was titrated into a reaction mixture containing FVIIIa in the presence of PSPCPE vesicles, reactions initiated with addition of APC, and the effects on cleavage of the A1 subunit at Arg^{336} monitored by Western blotting using 58.12 antibody that recognizes the N-terminal sequence of the A1 domain (Fig 3 inset). The addition of FX resulted in inhibition of cleavage at Arg^{336} in a concentration-dependent manner. Ratios of band densities of cleaved/intact A1subunit were used to estimate an apparent K_i of 105 ± 6 nM for this protective effect of FX (Fig 3). Taken together, these data suggested that residues contributing to the APC binding site in the FVIII A3 domain of FVIII participate in the interaction with FX.

Effect of the 2007–2016 Peptide on the FVIII LC and FX Interaction

Residues 2007–2016 (HAGMSTLFLV) in the A3 domain of FVIII LC have been demonstrated to contain a binding site for APC (20). The above results would suggest this sequence also contributes to FX binding. To determine the specificity of this sequence for FX interaction, we examined the effects of the 2007–2016 peptide on FVIII LC binding to FX using the ELISA-based assay (Fig 4A). Various concentrations of the 2007–2016 peptide in the presence of FVIII LC (200 nM) were incubated with FX (50 nM) that had been immobilized on microtiter wells, and bound FVIII LC was detected using a biotinylated anti-FVIII LC antibody (antibody 10104). The peptide inhibited the FVIII LC and FX interaction in a concentration-dependent manner with ~80% inhibition observed at the maximum peptide concentration employed (800 μM). An apparent K_i value of 152 ± 29 μM was obtained from the fitted curve. In contrast, control experiments using a scrambled sequence peptide (FTAVLHMLGS) showed little if any inhibition of binding. These findings were consistent with residues 2007–2016 in the A3 domain contributing to a FX binding site.

Binding of the 2007–2016 peptide to FX

To obtain the evidence that residues 2007–2016 in the A3 domain contains a FX-interactive site, direct binding between this peptide and FX was quantified using SPR-based assays. The peptide and FX interacted with low affinity, and it was difficult to determine reliable K_d values from the kinetic parameters. Therefore, maximum response units (RU) determined by the addition of various concentrations of peptide were used for calculation. These RU values

increased in a concentration-dependent manner, and the data were well-fitted using a single-site binding model (Fig 4B) to yield a K_d value of 7.7 ± 2.3 μM. In contrast, a control peptide with a scrambled sequence demonstrated little binding.

Direct binding of the peptide to FX was also established using EDC cross-linking. FX (200 nM) in the presence of biotinylated 2007–2016 peptide (200 μM) was incubated with various amounts of EDC at 23 °C for 2 hours. The 2007–2016 peptide and FX formed a cross-linked product of approximately 60 kDa that increased in intensity with increasing concentrations of EDC (Fig 4C, panel a) or increasing concentrations of peptide (Fig 4C, panel b). The mass of the adduct formed (~60 kDa) was consistent with a 1:1 stoichiometry of the peptide (~1.3 kDa) and FX (~59 kDa). Control experiments using BSA showed that no cross-linked product was formed (data not shown). The specificity of the interaction between the 2007–2016 peptide and FX was examined using unlabeled peptide as a competitor to block formation of the biotinylated peptide-FX adduct. Increasing concentrations of unlabeled peptide were combined with fixed concentration of FX (150 nM) and biotinylated peptide (100 μM), and the mixtures were reacted with EDC (2 mM) as above. Figure 4C, panel c illustrates the loss of biotinylated product following titration with the unlabeled 2007–2016 peptide. Together, these results directly identify residues 2007–2016 in the A3 domain as contributing to FX binding.

Binding of Recombinant A3C1C2 Mutants to FX

The above experiments strongly suggested that A3 residues 2007–2016 contain a FX-interactive site. In an attempt to identify the A3 residues that are responsible for interacting with FX, a series of recombinant FVIII mutants were prepared in which selected residues within this sequence were replaced with alanine. These variants were treated with thrombin and the A3C1C2 subunits purified as described in *Methods*. The interaction of FX and A3C1C2 variant subunits was evaluated using SPR. Affinity values were determined as described above and results are summarized in Table 1. The K_d for wild type A3C1C2 was 57.0 ± 4.8 nM, a value that was somewhat lower than that determined for intact FVIII light chain and may suggest increased FX affinity following removal of the a3 segment by thrombin. Binding of two A3C1C2 subunit variants, Thr2012Ala and Phe2014Ala, to FX showed 1.5- and 1.8-fold reduced affinity, respectively, compared to the wild type value. Based upon these observations, we also prepared double and triple mutants (Thr2012Ala/Phe2014Ala and Thr2012Ala/Leu2013Ala/Phe2014Ala) to further assess the contributions of these residues to binding. Thr2012Ala/Phe2014Ala and Thr2012Ala/Leu2013Ala/Phe2014Ala variants showed similar increases (3.6- and 4.2-fold, respectively) in K_d compared to the wild type value that were greater than the individual mutations, suggesting an additive effect of the mutations at Thr2012 and Phe2014.

Michaelis-Menten Analysis of FXase Using FVIII Mutants

The above variant FVIII forms were assessed in FXa generation assays where FX was titrated to assess K_m and V_{max} parameters. 1 nM FVIII wild type and mutant forms were activated by thrombin, reacted with 40 nM FIXa, and 20 μM PSPCPE, and reactions were initiated with varying amounts of FX (0–500 nM) as described in *Methods*. The results are presented in Figure 5 and summarized Table 2. Overall, Ala mutations within this sequence showed somewhat varied effects on V_{max}. The only single mutation yielding an appreciable effect on K_m differing from WT was at residue Thr2012 which resulted in a 1.6-fold increase in this parameter. However, the K_m for FX for the Thr2012Ala/Phe2014Ala and Thr2012Ala/Leu2013Ala/Phe2014Ala variants appeared to be somewhat further increased (~2.0- and ~4.0-fold compared with wild type, respectively).

The COOH-terminal region of the A1 subunit contains a primary binding site for FX (13). To eliminate the effect of interaction between FX and FVIII A1 domain, we prepared the A3C1C2 subunit from each of the recombinant FVIII mutants and reconstituted the A3C1C2 (10 nM) with WT A2 subunit (100 nM) as described under *Materials and Methods* to form an A2/A3C1C2 dimer lacking A1 subunit. Similar to the above experiments, A2/A3C1C2 dimer in the presence of 20 μM PSPCPE and FIXa (40 nM) was reacted with various concentrations of FX (0–500 nM) and rates of FXa generation were determined. Results are summarized in Table 2. Evaluation of the reconstituted dimer prepared from wild type A3C1C2 showed an ~10-fold reduction in V_{max} compared with intact FVIIIa whereas the K_m for FX was essentially unchanged. Mutations of residues Thr2012 and Phe2014 to alanine resulted in 2.1- and 2.2-fold increases in K_m compared with wild type, respectively. Furthermore, the K_m values for the Thr2012Ala/Phe2014Ala double mutant and Thr2012Ala/Leu2013Ala/Phe2014Ala triple mutant were increased 2.7- and 4.2-fold, respectively compared with wild type while V_{max} values were only appreciable affected. Overall, these results suggest a contribution of these residues to the K_m for substrate FX conversion.

DISCUSSION

In an earlier study, we identified a FX-binding site showing ~μM affinity within the A1 subunit of FVIIIa that was localized to the COOH-terminal acidic region (13). However, the contribution of FVIII LC (A3C1C2 domains) to binding FX was not determined. In the present study, we further investigated the potential for association between FVIII LC and FX, and present several lines of evidence in support of a direct interaction. Binding of FVIII LC to immobilized FX was observed in the absence of FIXa and phospholipid vesicles using ELISA and SPR-based assays. These results were supported by the formation of a covalent crosslink between FX and FVIII LC following chemical cross-linking by EDC. Competition of active site-modified APC and of a FVIII peptide derived from a previously identified APC-interactive site (20) to FX binding LC suggested that A3 domain residues 2007–2016 contributed to the FX binding site in LC. A role for this sequence was supported by analysis of recombinant FVIII variants where replacement of selected residues within this sequence with Ala yielded reduced affinity of the LC derived from the variants as well as an increase in K_m for FX using FXase comprised of these variants.

Our original study (13) identifying the A1 domain of HC and A1 subunit of FVIIIa as containing a FX-interactive site relied on the ELISA-based assay, which employed an anti-LC monoclonal antibody to capture FVIII or the A1/A3C1C2 subunit to the microtiter well. However, that study failed to show appreciable binding of FX to isolated LC. The reason(s) for this are not clear, but may have reflected initial formation of a LC-antibody complex that blocked subsequent reaction with added FX. In the present study, the ELISA-based assay was complemented by SPR and separate experiments were performed utilizing either FX or LC as the immobilized ligand. Results from these studies yielded (apparent) K_d values ranging from ~100 to <400 nM, suggesting sub-μM affinity for the FX-FVIII LC interaction. Thus this binding site in FVIII LC may represent a dominant FX site in FVIIIa given an apparent K_d of ~1–3 μM determined for the FX site in the A1 domain (13).

Studies by O'Brien et al (26) demonstrated that FX reduced the rate of FVIIIa inactivation and cleavage at Arg^{336} catalyzed by APC. Since an APC-binding site in FVIII was identified in FVIII LC within residues 2007–2016 of the A3 domain (20), these observations together suggested that sites in the LC for APC and FX may be overlapping. Indeed, we observed that active site-modified APC effectively competed for FX binding to LC resulting in ~90% inhibition of FX binding as judged by the ELISA-based assay. Conversely, FX blocked APC-catalyzed proteolysis of FVIIIa at Arg^{336} in a concentration-dependent

manner. The estimated K_i values were similar (~100 nM) in both types of assays, and approximated the K_d value for the FX-LC interaction, suggesting similar affinity values of APC and FX for FVIII LC. This FX-dependent inhibition of proteolytic cleavage by APC may contribute to the persistence of FVIIIa and subsequent FXase activity during the propagation phase of coagulation.

Similar to the FX site in A1 (13), the FVIII LC yielded a covalent complex with FX following reaction with the zero-length cross-linker, EDC. This reagent initially reacts with the carboxyl group or a carboxylic acid residue to form an unstable *O*-acylisourea adduct which can react with a nearby ε-amino group of Lys or hydroxyl group of nucleophiles such as Ser or Thr to form an isoamide or ester linkage (27). Furthermore, the synthetic peptide representing the 2007–2016 sequence also yielded a cross-linked product with FX. Evaluation of the residues in this peptide suggest a limited number of sites where cross-linking could occur and these are restricted to the hydroxyl groups of Ser2011 and/or Thr2012 as well as the COOH-terminus.

These two residues appear to reside at or near the FX-interactive site. Mutagenesis of Thr2012 or Phe2014 to Ala resulted in modest decreases (~1.5- and ~2-fold, respectively) in the affinity of the derived FVIII LC's for FX as judged by SPR. A double mutant where both residues were replaced by Ala and triple mutant (Thr2012Ala/Leu2013Ala/Phe2014Ala) yielded 3.6- and 4.2-fold increases in K_d, respectively, suggesting contribution of both residues to the binding interaction. In addition to demonstrating effects on binding, the Thr2012Ala mutation resulted in a slight increase (~50%) in the K_m of FXase for FX. Although no effect on this parameter was observed for the Phe2014Ala variant, when this mutation was combined with the Thr2012Ala, the double and triple mutants showed an apparent ~2- and ~4-fold increase in K_m, respectively, suggesting a possible synergy in effect. Furthermore, while the A2/A3C1C2 dimer is not a physiological relevant FVIII form, results obtained using these reagents revealed K_m values for the double and triple mutants that were also increased (~3- and ~4-fold of wild type, respectively), supporting a contribution of The2012Ala and Phe2014Ala to K_m and overall catalytic efficiency.

Little structural information is available regarding the 2007–2016 sequence in FVIII. The intermediate resolution X-ray structures (28, 29) show that this site resides on the opposite face of the A3 domain as residues 1811–1818, a sequence shown to be involved in the interaction with FIXa (30). Thus one could envision the A3 domain as serving as a bridge in binding enzyme and substrate during catalysis by FXase. However, this sequence, and in particular residues 2012–2014 appear to be somewhat masked by the A1 domain in the FVIII procofactor. We have previously presented evidence for new hydrogen bonding interactions formed between A1-A2 and A2-A3 domains resulting from activation of FVIII to FVIIIa (31). We speculate that procofactor activation may expose this FX site possibly following formation of new hydrogen bonding interactions.

In conclusion, we present evidence identifying a FX-interactive site within the sequence 2007–2016 of the A3 domain of FVIII that overlaps with a site for APC. LC residues Thr2012 and Phe2014 within this sequence appear to contribute to the FX binding interaction, as well as to the apparent catalytic efficiency of FXase by affecting the K_m for substrate FX.

Acknowledgments

We thank Amy E. Griffiths and Jennifer P. DeAngelis for excellent technical assistance. A preliminary account of this work was presented at the 23rd Congress of the International Society on Thrombosis and Haemostasis, July 25, 2011, Kyoto, Japan.

References

1. Mann KG, Nesheim ME, Church WR, Haley P, Krishnaswamy S. Surface-dependent reactions of the vitamin K-dependent enzyme complexes. Blood. 1990; 76:1–16. [PubMed: 2194585]
2. Miyahara N, Shoda J, Ishige K, Kawamoto T, Ueda T, Taki R, Ohkohchi N, Hyodo I, Thomas MB, Krishnamurthy S, Carraway KL, Irimura T. MUC4 interacts with ErbB2 in human gallbladder carcinoma: potential pathobiological implications. Eur J Cancer. 2008; 44:1048–1056. [PubMed: 18397823]
3. Vehar GA, Keyt B, Eaton D, Rodriguez H, O'Brien DP, Rotblat F, Oppermann H, Keck R, Wood WI, Harkins RN, et al. Structure of human factor VIII. Nature. 1984; 312:337–342. [PubMed: 6438527]
4. Andersson LO, Forsman N, Huang K, Larsen K, Lundin A, Pavlu B, Sandberg H, Sewerin K, Smart J. Isolation and characterization of human factor VIII: molecular forms in commercial factor VIII concentrate, cryoprecipitate, and plasma. Proc Natl Acad Sci U S A. 1986; 83:2979–2983. [PubMed: 3085106]
5. Fay PJ, Anderson MT, Chavin SI, Marder VJ. The size of human factor VIII heterodimers and the effects produced by thrombin. Biochim Biophys Acta. 1986; 871:268–278. [PubMed: 3085715]
6. Eaton D, Rodriguez H, Vehar GA. Proteolytic processing of human factor VIII. Correlation of specific cleavages by thrombin, factor Xa, and activated protein C with activation and inactivation of factor VIII coagulant activity. Biochemistry. 1986; 25:505–512. [PubMed: 3082357]
7. Fay PJ, Mastri M, Koszelak ME, Wakabayashi H. Cleavage of factor VIII heavy chain is required for the functional interaction of a2 subunit with factor IXA. J Biol Chem. 2001; 276:12434–12439. [PubMed: 11278520]
8. Regan LM, Fay PJ. Cleavage of factor VIII light chain is required for maximal generation of factor VIIIa activity. J Biol Chem. 1995; 270:8546–8552. [PubMed: 7721754]
9. Donath MS, Lenting PJ, van Mourik JA, Mertens K. The role of cleavage of the light chain at positions Arg1689 or Arg1721 in subunit interaction and activation of human blood coagulation factor VIII. J Biol Chem. 1995; 270:3648–3655. [PubMed: 7876103]
10. Nogami K, Wakabayashi H, Fay PJ. Mechanisms of factor Xa-catalyzed cleavage of the factor VIIIa A1 subunit resulting in cofactor inactivation. J Biol Chem. 2003; 278:16502–16509. [PubMed: 12606556]
11. Koszelak Rosenblum ME, Schmidt K, Freas J, Mastri M, Fay PJ. Cofactor activities of factor VIIIa and A2 subunit following cleavage of A1 subunit at Arg336. J Biol Chem. 2002; 277:11664–11669. [PubMed: 11799130]
12. Nogami K, Wakabayashi H, Schmidt K, Fay PJ. Altered interactions between the A1 and A2 subunits of factor VIIIa following cleavage of A1 subunit by factor Xa. J Biol Chem. 2003; 278:1634–1641. [PubMed: 12426309]
13. Lapan KA, Fay PJ. Localization of a factor X interactive site in the A1 subunit of factor VIIIa. J Biol Chem. 1997; 272:2082–2088. [PubMed: 8999906]
14. Lamphear BJ, Fay PJ. Proteolytic interactions of factor IXa with human factor VIII and factor VIIIa. Blood. 1992; 80:3120–3126. [PubMed: 1467518]
15. Walker FJ, Fay PJ. Regulation of blood coagulation by the protein C system. FASEB J. 1992; 6:2561–2567. [PubMed: 1317308]
16. Eaton DL, Wood WI, Eaton D, Hass PE, Hollingshead P, Wion K, Mather J, Lawn RM, Vehar GA, Gorman C. Construction and characterization of an active factor VIII variant lacking the central one-third of the molecule. Biochemistry. 1986; 25:8343–8347. [PubMed: 3030393]
17. Fay PJ, Smudzin TM, Walker FJ. Activated protein C-catalyzed inactivation of human factor VIII and factor VIIIa. Identification of cleavage sites and correlation of proteolysis with cofactor activity. J Biol Chem. 1991; 266:20139–20145. [PubMed: 1939075]
18. Krishnaswamy S, Williams EB, Mann KG. The binding of activated protein C to factors V and Va. J Biol Chem. 1986; 261:9684–9693. [PubMed: 3755431]
19. Fay PJ, Walker FJ. Inactivation of human factor VIII by activated protein C: evidence that the factor VIII light chain contains the activated protein C binding site. Biochim Biophys Acta. 1989; 994:142–148. [PubMed: 2521291]

20. Walker FJ, Scandella D, Fay PJ. Identification of the binding site for activated protein C on the light chain of factors V and VIII. J Biol Chem. 1990; 265:1484–1489. [PubMed: 2136854]
21. Nogami K, Lapan KA, Zhou Q, Wakabayashi H, Fay PJ. Identification of a factor Xa-interactive site within residues 337–372 of the factor VIII heavy chain. J Biol Chem. 2004; 279:15763–15771. [PubMed: 14764590]
22. Wakabayashi H, Koszelak ME, Mastri M, Fay PJ. Metal ion-independent association of factor VIII subunits and the roles of calcium and copper ions for cofactor activity and inter-subunit affinity. Biochemistry. 2001; 40:10293–10300. [PubMed: 11513607]
23. Ansong C, Fay PJ. Factor VIII A3 domain residues 1954–1961 represent an A1 domain-interactive site. Biochemistry. 2005; 44:8850–8857. [PubMed: 15952791]
24. Nogami K, Zhou Q, Myles T, Leung LL, Wakabayashi H, Fay PJ. Exosite-interactive regions in the A1 and A2 domains of factor VIII facilitate thrombin-catalyzed cleavage of heavy chain. J Biol Chem. 2005; 280:18476–18487. [PubMed: 15746105]
25. Lollar P, Fay PJ, Fass DN. Factor VIII and factor VIIIa. Methods Enzymol. 1993; 222:128–143. [PubMed: 8412790]
26. O'Brien LM, Mastri M, Fay PJ. Regulation of factor VIIIa by human activated protein C and protein S: inactivation of cofactor in the intrinsic factor Xase. Blood. 2000; 95:1714–1720. [PubMed: 10688829]
27. Carraway KL, Koshland DE. Carbodiimide modification of proteins. Methods Enzymol. 1972; 25:616–623.
28. Ngo JC, Huang M, Roth DA, Furie BC, Furie B. Crystal structure of human factor VIII: implications for the formation of the factor IXa-factor VIIIa complex. Structure. 2008; 16:597–606. [PubMed: 18400180]
29. Shen BW, Spiegel PC, Chang CH, Huh JW, Lee JS, Kim J, Kim YH, Stoddard BL. The tertiary structure and domain organization of coagulation factor VIII. Blood. 2008; 111:1240–1247. [PubMed: 17965321]
30. Lenting PJ, van de Loo JW, Donath MJ, van Mourik JA, Mertens K. The sequence Glu1811-Lys1818 of human blood coagulation factor VIII comprises a binding site for activated factor IX. J Biol Chem. 1996; 271:1935–1940. [PubMed: 8567641]
31. Wakabayashi H, Fay PJ. Identification of residues contributing to A2 domain-dependent structural stability in factor VIII and factor VIIIa. J Biol Chem. 2008; 283:11645–11651. [PubMed: 18299331]

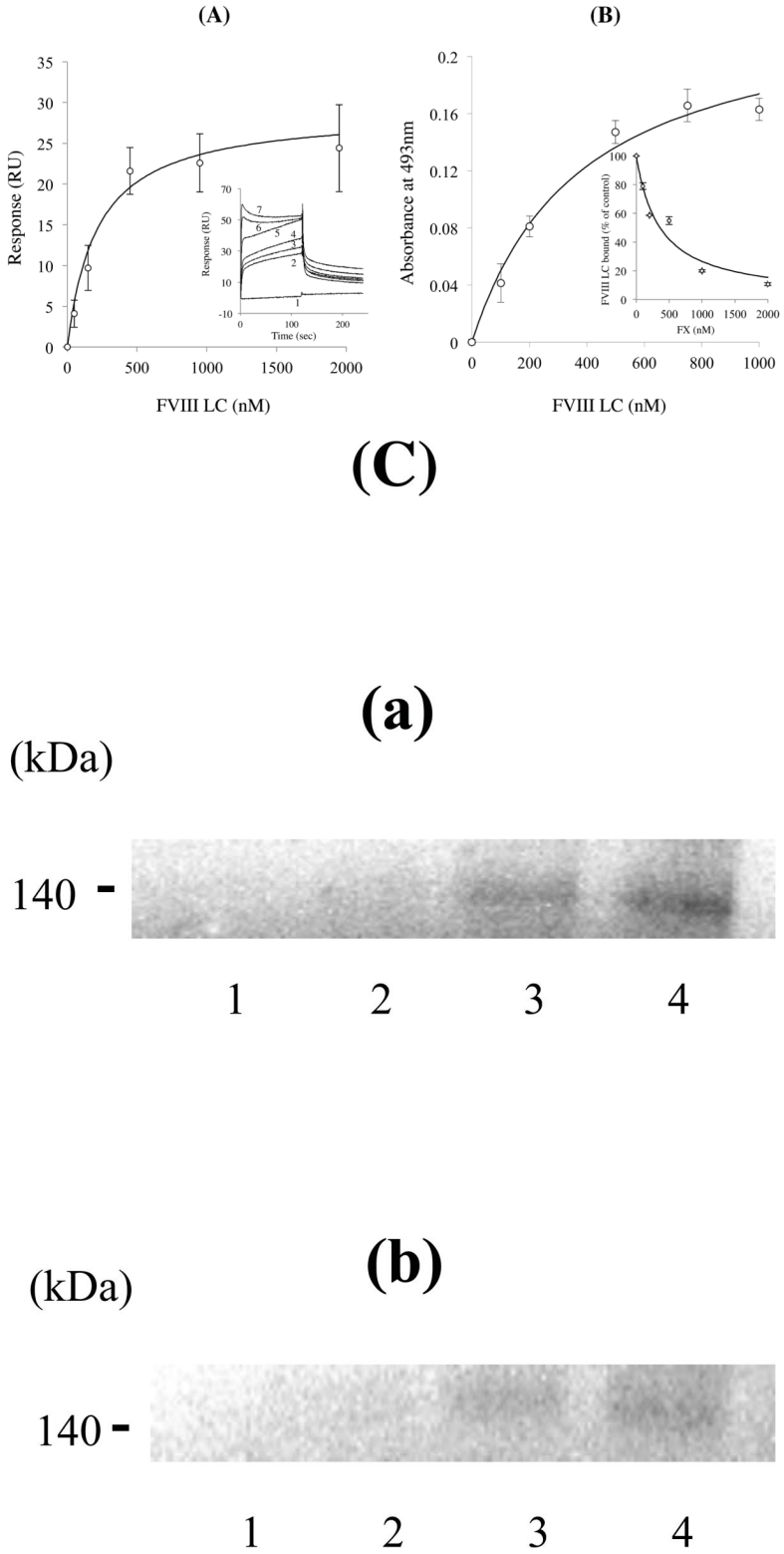

Figure 1. Binding of FVIII LC to FX

A) Binding of FVIII LC to FX by SPR. Maximum RU values at equilibrium for association of FVIII LC were plotted as a function of FVIII LC, and the data were fitted using the

Equation 1 according to a single-site binding model. Experiments were performed at least three separate times and mean values are shown. Inset: Curves 1–7 show representative association/dissociation curves for FVIII LC (0, 50, 100, 200, 500, 1000 and 2000 nM, respectively. B) Binding of FVIII LC to FX by ELISA-based assays. Various concentrations of FVIII LC were reacted with FX (50 nM) immobilized onto microtiter wells. Bound FVIII LC was detected using a biotinylated anti-FVIII LC antibody, 10104. Data were fitted using the Equation 1 (single-site biding model). Inset: Mixtures of FVIII LC (500 nM) and various concentrations of FX were incubated with immobilized FX. Absorbance value corresponding to FVIII LC binding to FX in the absence of competitor was defined as 100%. The data were fitted by non-linear least squares regression using Equation 2 (competitive inhibition model). Experiments were performed at least three separate times and mean values are shown. C) EDC cross-linking of FVIII LC and FX. FVIII LC (200 nM) was reacted with FX (200 nM) in the presence of various concentrations of EDC (lanes 1–4; 0, 1, 2, and 5 mM, respectively) at 23 °C for 2 hours, followed by immunoblotting using the anti-FVIII LC antibody, 2D2 (panel a) or the anti-FX antibody (panel b). Experiments were performed at least three separate times and typical results are shown.

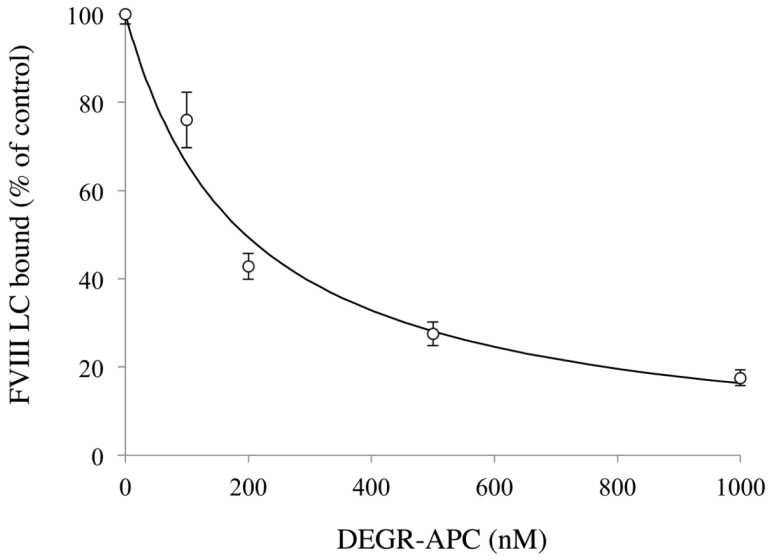

Figure 2. Inhibition of FVIII LC and FX binding by DEGR-APC

FVIII LC (500 nM) was incubated with FX-coated wells (50 nM/well) in the presence of various concentrations of DEGR-APC. Bound FVIII LC was detected using a biotinylated anti-FVIII LC antibody, 10104. The absorbance value corresponding to FVIII LC bound to FX in the absence of DEGR-APC was defined 100%. The percentage of FVIII LC was plotted as a function of DEGR-APC concentration, and the data were fitted by nonlinear least squares regression using Equation 2 (competitive inhibition model). Experiments were performed at least three separate times and mean values are shown.

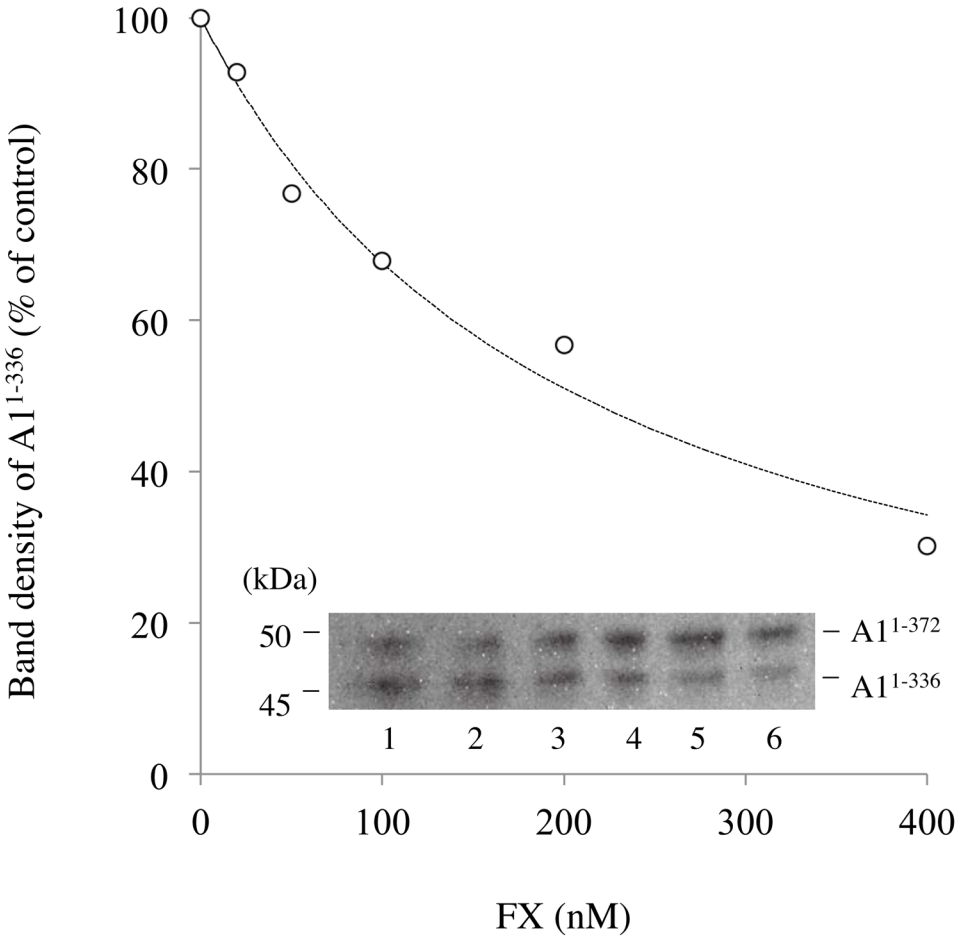

Figure 3. Effect of FX on A1 cleavage at Arg^{336} by APC

Mixtures of FVIIIa (130 nM) and various concentrations of FX were incubated with APC (2 nM) and PSPCPE (100 μM) in HBS-buffer containing 2 mM $CaCl_2$ for 10 min. Samples were run on 8% gels followed by Western blotting using an anti-A1 monoclonal antibody, 58.12. Inset: Lanes 1–6 show the A1 cleavage of FVIIIa in the presence of FX (0, 20, 50, 100, 200, and 400 nM, respectively). The graph shows quantitative densitometry of the A1^{336} product. Density values of A1^{336} generated by APC cleavage in the absence of FX were used to represent the 100% level. Data were fitted by nonlinear least squares regression using Equation 2 (competitive inhibition model) and shown as a dashed line. Experiments were performed at least three separate times and typical results are shown.

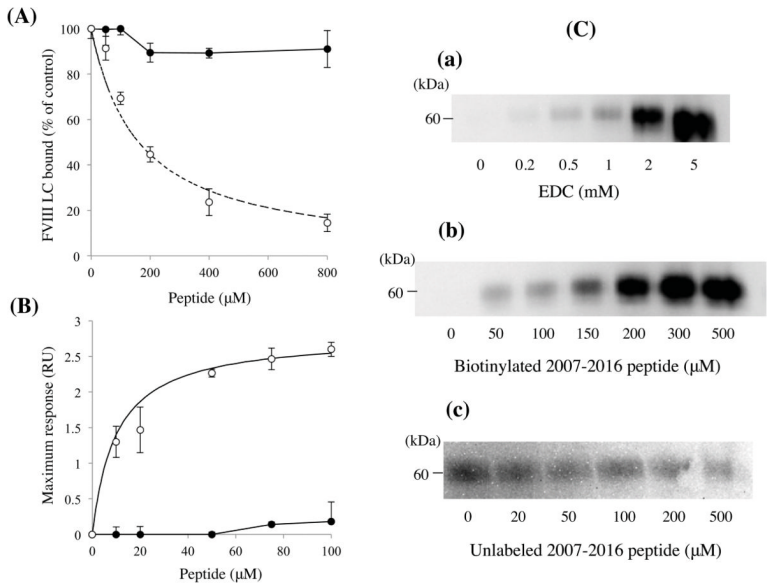

Figure 4.

(A) Effect of 2007–2016 peptide on FVIII LC binding to FX. FVIII LC (200 nM) was mixed with various concentrations of the 2007–2016 peptide (open circles) or scrambled sequence peptide (closed circles) and mixtures were then incubated with immobilized FX (50 nM). Bound FVIII LC was detected using a biotinylated anti-FVIII LC antibody. The absorbance value corresponding to FVIII LC binding to FX in the absence of competitor was defined as 100%. The data were fitted (dashed line) by non-linear least squares regression using Equation 2 (competitive inhibition model). Experiments were performed at least three separate times and mean values are shown. **(B) Direct binding of 2007–2016 peptide to FX as determined by SPR.** Various amounts of the 2007–2016 peptide (open circles) or scrambled sequence peptide (closed circles) were injected onto a sensor chip containing immobilized FX for 2 minutes, followed by a change to running buffer for 2 minutes. Maximum values for association of the peptide were plotted as a function of peptide concentration, and the data were fitted using the Equation 1 (single-site binding model). Experiments were performed at least three separate times and mean values are shown.

(C) EDC cross-linking of 2007–2016 peptide and FX. Panel a) FX (200 nM) was incubated with biotinylated 2007–2016 peptide (200 μM) in the presence of indicated concentrations of EDC at 23 °C for 2 hours, followed by immunoblotting using streptavidin. Panel b) Cross-linked products formed with FX (200 nM) and indicated concentrations of the 2007–2016 peptide with EDC (2 mM). Panel c) FX (150 nM) and biotinylated 2007–2016 peptide (100 μM) reacted with EDC (2 mM) in the presence of indicated concentrations of the unlabeled 2007–2016 peptide and were immunoblotted. Experiments were performed at least three separate times and typical results are shown.

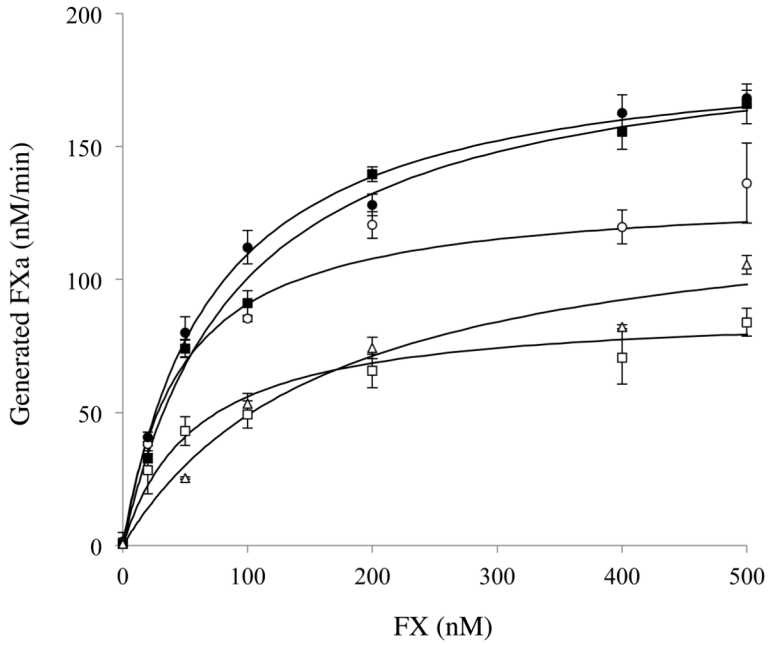

Figure 5. Michaelis-Menten Analysis of FXase formed using FVIII LC mutants

FVIII (1 nM) was activated by thrombin (30 nM) for 1 minute in the presence of 20 μM PSPCPE. FXa generation was initiated by the addition of FIXa (40 nM) and various concentrations of FX (0–500 nM) as described in Methods. The symbols used are as follows; wild type (open circles), Thr2012Ala (closed circles), Phe2014Ala (open squares), Thr2012Ala/Phe2014Ala (closed squares), and Thr2012Ala/Leu2013Ala/Phe2014Ala (open triangles). Experiments were performed at least three separate times and mean values are shown.

Table 1

Binding parameters for the interaction of A3C1C2 mutants and FX determined by SPR

A3C1C2 form	K_d
	nM
Wild type	57.0 ± 4.8
Met2010Ala	59.5 ± 0.8
Ser2011Ala	59.4 ± 3.3
Thr2012Ala	85.8 ± 2.9†
Leu2013Ala	63.9 ± 12.0
Phe2014Ala	104 ± 4†
Leu2015Ala	45.1 ± 10.0
Val2016Ala	55.7 ± 7.2
Thr2012Ala/Phe2014Ala	193 ± 21†
Thr2012Ala/Leu2013Ala/Phe2014Ala	239 ± 22†

Reactions were performed as described under *Materials and Methods*. Parameter values ± standard deviations were calculated by nonlinear regression analysis using the evaluation software provided by GE Healthcare.

† $P < 0.01$ compared with the value for wild type.

Table 2

Kinetics parameters for FXa generation by FXase with FVIII mutants

FVIII form	K_m	V_{max}
	nM	*nM·min*$^{-1}$
Wild type	46.6 ± 6.0	133 ± 5
Met2010Ala	48.0 ± 4.1	76.0 ± 10.0†
Ser2011Ala	36.4 ± 5.1	109 ± 4†
Thr2012Ala	72.6 ± 8.4*	189 ± 6†
Leu2013Ala	46.8 ± 3.2	129 ± 3
Phe2014Ala	58.5 ± 7.3	88.7 ± 6.8†
Leu2015Ala	46.1 ± 5.1	120 ± 4
Val2016Ala	39.3 ± 5.4	151 ± 12
Thr2012Ala/Phe2014Ala	93.2 ± 16.3*	194 ± 12†
Thr2012Ala/Leu2013Ala/Phe2014Ala	168 ± 26.4†	131 ± 15
Reconstituted A2/A3C1C2 form	K_m	V_{max}
	nM	*nM·min*$^{-1}$
Wild type	29.5 ± 2.0	14.1 ± 0.8
Thr2012Ala	62.6 ± 5.7†	12.7 ± 0.3
Phe2014Ala	63.7 ± 6.2†	7.6 ± 0.4
Thr2012Ala/Phe2014Ala	78.4 ± 4.5†	12.9 ± 2.0
Thr2012Ala/Leu2013Ala/Phe2014Ala	124 ± 21†	9.8 ± 1.5

Reactions were performed as described under *Materials and Methods*. K_m and V_{max} values ± standard deviations were calculated by Michaelis-Menten kinetics.

$^{*}P < 0.05$ or

$^{\dagger}P < 0.01$ compared with the value for wild type.